

## INVESTIGATIONS OF EVAPORATED FRONT CONTACTS ALONG THE GRAIN BOUNDARIES OF MULTICRYSTALLINE SILICON SOLAR CELLS

V. Schlosser<sup>1</sup>, R. Ebner<sup>2</sup>, W. Markowitsch<sup>1</sup>, P. Bajons<sup>1</sup>, G. Klinger<sup>3</sup>, A. A. El-Amin<sup>1</sup>, J. Summhammer<sup>2</sup>

<sup>1</sup> Institut für Materialphysik der Universität Wien, A-1090 Wien, Strudlhofgasse 4, Austria

<sup>2</sup> Atominstitut der Österreichischen Universitäten, A-1020 Wien, Stadionallee 2, Austria.

<sup>3</sup> Institut für Meteorologie und Geophysik der Universität Wien, A-1090 Wien, Althanstraße 14, Austria.

**ABSTRACT:** A series of sets of multicrystalline silicon solar cells have been prepared. One cell of each set was equipped with a front contact grid along the grain boundaries. A second cell was equipped with the same grid but rotated by 90 degrees and onto the third cell a geometrical standard grid was applied. The grids were either prepared by plotting silver ink lines and subsequent burn in or by photolithographically structured Ni/Ag layers deposited by evaporation or a galvanic process. No passivation or protection against reflection losses were applied. A statistical evaluation of the solar cell parameters for two illumination intensities in a temperature range between 295 K and 330 K was done. At room temperature the gain of maximum output power for cells with the grid on the grain boundaries for high and low light intensities was 1.17 and 1.15, respectively, compared with cells having a standard grid. The average linear temperature coefficient for the power output was determined to be  $-0.80\%K^{-1}$  for cells with a grain boundary grid and  $-0.74\%K^{-1}$  for cells with a standard grid. For one cell prepared by the photolithographic method a maximum power output of more than  $10\text{ mWcm}^{-2}$  was observed under  $1\text{ kWm}^{-2}$  irradiation at ambient temperature.

Keywords: Silicon – 1: Multi-Crystalline – 2: Contact – 3.

### 1. INTRODUCTION

Most of the reduction of the conversion efficiency observed on solar cells made from multi-crystalline silicon – mc-Si – compared with single-crystalline solar cells can be attributed to the presence of grain boundaries. Generally the electronic structure of grain boundaries causes an enhanced recombination of minority carriers which results in a local reduction of the light generated current in the solar cell. Grain boundaries often act as a potential barriers for the majority carriers which undesirably raise resistance in the current path between the emitter of the solar cell and the metal fingers of the front contact. In order to reduce the unwanted effects of grain boundaries previously a novel front contact grid which is applied onto the grain boundaries was proposed [1]. Two major benefits were expected when a grain boundary oriented finger contact (GBOF) is applied to a mc-Si solar cell. These recently have been demonstrated : (i) The light shading of the metal grid affects mainly areas with a low quantum yield and (ii) the total series resistance can be significantly lowered compared to solar cells which have a conventional geometric front contact grid. [2,3]. These effects lead to an increase in the short circuit current density, the curve fill factor and as a result in the output power. Previously, an automated method was developed which allowed the individual determination of the grid structure for each wafer prior to the application of the front metal grid. A more detailed description is given elsewhere [4]. After the formation of the pn-junction and the metalisation of the backside the grid was automatically plotted using silver ink onto the emitter of the cell and burnt in. The purpose of this work was to extend the previous investigations to different ambient conditions. The results enable us to estimate the physical limitations of the present preparation technique of the GBOF contact and to evaluate an improved front contact procedure. In this work only a part of all the cells processed so far – cells of group B in [3] – are investigated. Therefore the statistical results can be different in some cases.

### 2. EXPERIMENTAL

#### 2.1 Solar cell preparation

A series of either pairs or triplets of solar cells prepared from adjacent mc p-Si wafers by thermal diffusion from a liquid phosphorous source were used to statistically evaluate the solar cell parameters. Except for the front side contact all processing was done identically. Two or three different metal grids were applied to the cell pairs or triplets respectively. Extreme care was taken to ensure that the total area covered by the front contact was the same for each set. The contact area for a theoretically optimum grid depends on the emitter's sheet resistance which determines the maximum allowable spacing between lines and the linewidth of the metal fingers. Assuming a homogenous sheet resistance over the whole wafer a best fitting line spacing for a rectangular grid can be derived. The resulting metal area was kept constant for all grids. For the majority of the cells the front grid was made by plotting a silver ink with suitable consistency onto the emitter and a subsequent burn in. For a few cells a photolithographic lift off process was used to deposit Ni/Ag contacts by thermal evaporation or galvanic procedures. Currently, these cells are too few to allow a statistical data interpretation.

The wafers were supported by either Baysix or Euro-solare. Saw damage removal and surface cleaning was done chemically by either hydroxide based or acid based solutions. The diffusion was carried out in an open tube furnace suitable to process 20 wafers a time. Typically the final average sheet resistance was between  $25\ \Omega/$  and  $35\ \Omega/$ . Pairs and triplets were placed in subsequent positions so that the sheet resistance do not significantly vary. After the diffusion step the backside of the cells were fully metallised by screen printing an Al/Ag- paste and burning in. One cell of a pair or of a triplet, which nearly always have a very similar grain structure and therefore can be expected to have similar electrical properties, was equipped with a front grid preferentially along the grain boundaries. These cells will be referred to as ON-cells later on. Prior to the application of the grid, the grain boundaries

were identified by the optical contrast of the grains with a resolution of 50  $\mu\text{m}$ . Then the grid was plotted computer controlled with silver ink according to the optical contrast image along a part of the grain boundaries. The selection of the covered grain boundaries was done with respect of the line density and the total area of optical shadowing. The aperture of the dispensing tube was 250  $\mu\text{m}$  and the plotting accuracy 25  $\mu\text{m}$ . When the silver ink was dry it was burnt in. In the case of evaporated/galvanic contacts a 1:1 mask of the calculated grid was generated. Photolithography was done by placing the mask on top of the cell's surface which was spin coated with a photoresist and exposed to light. After developing the remaining photoresist covered all areas which should not be metallised. The bare silicon surface was carefully washed and a thin layer of Ni was deposited either by thermal evaporation or by a galvanic deposition step. After removing the photoresist and lifting off the excess metal the contacts were thickened in a galvanic silver bath to the desired cross section of the contact fingers.

For the second cell of each set the same grid was used, but, however, the wafer intentionally was misaligned by a rotation of 90 degrees before the grid was deposited in the same manner as described above. In this case only a small fraction of the total contact/emitter interface is placed on a grain boundary (OFF-cells). In the case of cell triplets the third cell obtained a standard H-grid consisting of parallel fingers and two busbars (STD-cells). Again a plotting procedure was used instead of a conventional screen printed grid since it turned out that screen printed lines had a lower aspect ratio which may increase the series resistance and thus influence the statistically evaluated solar cell parameters. After the application of the front contact the edges of the cells were mechanically abraded to remove short circuits across the pn-junction. Neither grain boundary nor surface passivation has been done so far and no optical coating was deposited for the minimisation of reflection losses.

## 2.2 Characterisation

At ambient temperature (18  $^{\circ}\text{C}$  – 22  $^{\circ}\text{C}$ ) the current-voltage characteristics was measured (i) in the dark, (ii) at a high illumination intensity of 1  $\text{kWm}^{-2}$  and (iii) at a low illumination intensity. In this case four 150 W tungsten bulbs with a colour temperature of about 3000 K were used to illuminate the samples. The high mismatch of the colour temperature compared to AM1.5 conditions ( $T_{col} \approx 5400$  K) was leading to a high IR intensity of the total spectrum. The irradiance measured with a pyranometer (wavelength range 0.2  $\mu\text{m}$  – 2.8  $\mu\text{m}$ ) was determined to be 213  $\text{Wm}^{-2}$  whereas the reference silicon cell from Solarex output a signal corresponding to a light intensity of 0.127 times AM1.5 irradiance. Additionally, at low illumination intensities and in the dark, the temperature variation of the current-voltage curves was recorded between 300 K and 330 K. Time-resolved infrared thermography on some selected cells was used to investigate the current density distribution in the contact fingers and at the contact/emitter interface. The experiments were done by applying a reverse biased pulse across the device. Temperature changes at the cell's surface were monitored with an AGEMA 570 thermal imaging system operating in a wavelength range between 7.5  $\mu\text{m}$  und 13  $\mu\text{m}$ . Up to 20 frames/s of 320x240 signals were taken. The temperature resolution was 50 mK and the lateral resolution 140  $\mu\text{m}$ .

## 3. RESULTS

The coverage of the cells surface with metal typically was between 8 % and 11 %. From the current-voltage curves under illumination the solar cell parameters, short circuit current density,  $j_{SC}$ , open circuit voltage,  $V_{OC}$ , curve fill factor,  $CFF$ , maximum output power per area,  $P_{max}$  and matched load resistance,  $R_L$  were derived for each cell. The average values of the parameters for each group of cell – ON, OFF, STD – were calculated. Only cells prepared by plotting silver ink lines are included. The current-voltage curve of an ON-cell without ARC made from an 105  $\text{cm}^2$  Eurosolare wafer in the dark and under low light intensity – 0.127  $\text{Wm}^{-2}$  – as a function of the temperature is shown in Fig.1. The results obtained for the measurements are summarised in Table I the upper half giving the results for high illumination intensity,  $P_{inc}$ , the lower those for the measurements at low intensities. All solar cell parameters of ON-cells are better than for STD- or OFF-cells for high illumination intensities which has been previously reported [3] as well as for low light intensities.

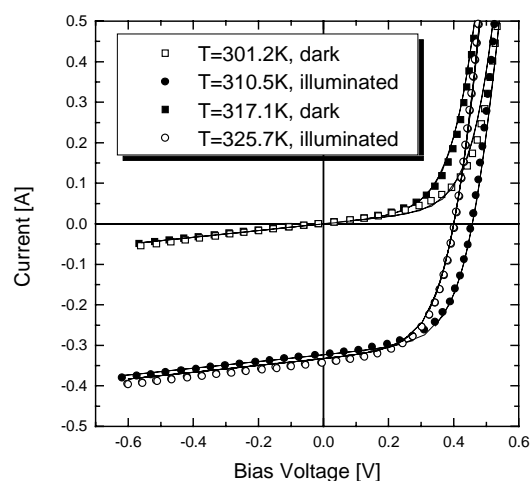


**Figure 1:** The measured current-voltage characteristics of a cell with the front metal grid along the grain boundaries (symbols). The lines show the result of a fit using one set of parameters.

**Table I:** Mean values of the solar cell parameters at two illumination levels taken at room temperature from cells with different front contact grids.

$P_{inc}$ $\text{kWm}^{-2}$	Type	$j_{SC}$ $\text{mAcm}^{-2}$	$V_{OC}$ V	$CFF$ %	$P_{max}$ $\text{mWcm}^{-2}$
1.000	ON	21.9	0.562	66.2	8.17
	OFF	21.3	0.560	63.3	7.56
	STD	20.6	0.544	62.1	6.96
0.127	ON	2.96	0.491	62.2	0.905
	OFF	2.88	0.485	59.1	0.831
	STD	2.77	0.470	60.3	0.786

A comparison of the ON- and the OFF- cells with the cells equipped with the geometrical standard H-pattern shows a gain in the output power of 1.17 for the ON-cells and of 1.09 for the OFF-cells at high light levels. This gain is reduced somewhat at low intensities to 1.15 and 1.06 respectively. Only the STD-cells are equipped with busbars for current collection which are believed to reduce the series resistance. However, once the cross section of the fingers is sufficiently large it appears that the network-like metal finger structure is superior for mc-Si cells regardless of the position of the lines with respect to grain boundaries. This is the reliable explanation for the fact that the OFF-cells with plotted contacts exhibit a higher output than STD-cells. In order to easily compare the temperature dependence of the solar cell parameters between 300 K and 330 K the variations always were approximated by a linear function of the temperature even when slight deviations from linearity were observed. The linear temperature coefficient for maximum power output,  $\alpha_p$  is defined as

$$\alpha_p = \frac{1}{P_{300}} \frac{\Delta P_{\max}}{\Delta T}$$

where  $P_{300}$  is the maximum power output at 300 K and  $\Delta P_{\max}$  is the change of the maximum output power over the temperature range  $\Delta T$ . In the same manner the coefficients for the short circuit current,  $\alpha_i$ , the open circuit voltage,  $\alpha_V$  and the curve fill factor,  $\alpha_{FF}$  are defined. The results are summarised in Table II.

**Table II:** Mean values of the linear temperature coefficients of the solar cell parameters for temperatures between 300 K and 330 K.

Type	$\alpha_i$	$\alpha_V$	$\alpha_{FF}$	$\alpha_p$
			% K <sup>-1</sup>	
ON	+0.23	-0.69	-0.33	-0.80
OFF	+0.24	-0.67	-0.20	-0.64
STD	+0.24	-0.70	-0.28	-0.74

No significant difference in the temperature dependence of the short circuit current and open circuit voltage was found. As expected, the first parameter increases slightly with temperature whereas the latter decreases. This confirms our assumption that the differently contacted cells are very similar in all electrical properties that are independent of the front side grid and therefore any noticeable differences can be attributed to the way the metal grid is applied.  $CFF$  as well as  $P_{\max}$ , however, decrease significantly stronger with temperature for ON-cells than for the other types of cells. Since we suspected that this is caused by different series resistance we tried to model the temperature dependence of the solar cell parameters. In a first step for some cells all current-voltage curves were fitted with one set of fit parameters assuming a single diode model which describes the recombination current across the junction. The result for an ON-cell are shown in Fig. 1. For a constant temperature the fit parameter were the light generated current,  $i_l$ , the saturation current,  $i_0$ , the series resistance,  $R_S$  and the shunt conductance,  $G_{SH}$ . Within the resolution of our fitting  $R_S$  and  $G_{SH}$  were practically independent of the temperature. The temperature dependence of the saturation current

obeyed a thermal activation law with an energy level somewhere between 0.5 eV on 0.8 eV. With the results of our fit in a first step the temperature dependence of the solar cell parameters was derived from the fitted current-voltage curves in order to verify the quality of the fit. If the calculated dependence was in good agreement with the experimentally observed all fit parameters except  $R_S$  were left unchanged. Varying  $R_S$  over a wide range leads to the result that the lower  $R_S$  the higher the decrease of  $CFF$  and  $P_{\max}$  with increasing temperature.

In Fig.2 the result of a thermography analysis for a silver ink processed ON-cell is shown. The cell was applied to a reverse biased voltage pulse for 200 ms. The image on the right side of Fig. 2 was obtained by taking the difference of the temperature signal between the cell without and with voltage stress. Therefore only the temperature increase due to the heating during pulse as a function of the position is observed. This method has the advantage that there is no need for corrections due to different emissivities or reflectance of the metal fingers and the silicon. In the left image the whole contact grid is displayed as lines of dark contrast on a grey shaded background which represents the emitter's surface. Some observable light grey lines arise from the etched surface structure which is caused by the chemical cleaning procedure. The contact finger from the lower left to the upper right of the image preferentially conducts most of the current. Although the metal itself remains cold due to the high thermal conductivity and the well cooled surface area the silicon below the contact is undesirably heated up. The reason for the reduced ability of the other fingers to conduct a proportional part of the total current is potentially caused by inhomogeneities in the lines due to the plotting process.

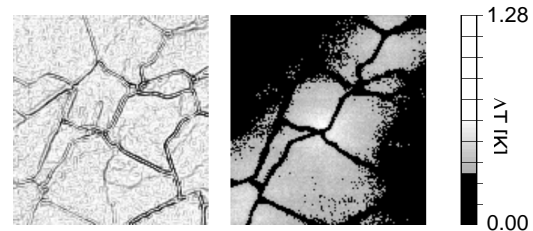


**Figure 2:** Contrast image of a part of a ON-cell's surface showing the silver ink covered grain boundaries (left) and an IR image showing the temperature increase during a reverse biased voltage pulse (right).

#### 4. CONCLUSIONS

Great care has been taken to prepare sets of mc-Si solar cells with structural and electronic properties as identical as possible. The final cells merely differed in the shape or orientation of the front metal grid. The investigations of the solar cell output from these cells, where the grid was prepared by plotting silver ink onto the emitter which subsequently was burnt in, showed that a grid design placed on grain boundaries yields an improved power output under different light and temperature conditions. At room temperature and high light levels this effect is the largest. All solar cell parameters,  $j_{SC}$ ,  $V_{OC}$  and  $CFF$ ,

exhibit an enhancement for ON-cells. The increase in the short circuit current can be attributed to the fact that less area with a high quantum yield is shaded. The improvement of  $CFI$  is caused by a reduction of the series resistance losses. On an average, the series resistance losses are reduced in ON-cells. This was confirmed by the observed smaller gain in power output at lower illumination intensities as well as for higher operating temperatures. This tendency agrees with the results of solar cell modelling. The rather large increase of the open circuit voltage however can not solely be described by the shift of the current-voltage characteristics due to the higher short circuit current. Presently, a rather speculative explanation is that the emitter's electrically active donor concentration in the grains differs somewhat from the concentration at the grain boundaries.

From thermographical mapping we learned that the limited control of the linewidth and aspect ratio and inhomogeneities during the drawing of the silver ink grid is leading to an unpredictable current density distribution in the final grid which may cause series resistance losses and long time instabilities. The disadvantages of the current procedure for the application of a selective metal grid are as follows:

- The selection of grain boundaries is merely optically and does not involve electrical criteria.
- The plotting of the lines with silver ink does not allow a precise control over the homogeneity and a variation of the cross section of the current collecting grid.
- The high temperature burn-in requires a deep pn-junction to avoid shunt effects by silver particles.

The substitution of the optical recognition system by a minority carrier lifetime mapping set-up is under progress. Evaporated and photolithographically shaped metal contacts allow a precise design with respect to the current paths and local current density distribution. Moreover, this method does not require a high temperature process which is favourable for improved pn-junction profiles. However a successful metallisation strongly depends on the surface cleaning prior to evaporation and the choice of a metal with a low contact resistance to the emitter. The ongoing work therefore primarily focuses on an improved metallisation process by a photolithographically structured, evaporated front grid which is thickened by galvanic silver deposition. Although we have successfully processed only a few cells, it is very encouraging that one of the cells with a grid on the grain boundaries showed a power output of more than  $10 \text{ mWcm}^{-2}$  even without antireflective coating and without any passivation process.

#### ACKNOWLEDGEMENT

This work was partly supported by the Fonds zur Förderung der Wissenschaftlichen Forschung (Project P14432) and by the Hochschuljubiläumsstiftung der Stadt Wien.

#### REFERENCES

[1] J. Summhammer, V. Schlosser, Proceedings 12<sup>th</sup> EC Photovoltaic Solar Energy Conference, H.S. Stevens (1994) 734.

[2] M. Radike, J. Summhammer, Proceedings 16<sup>th</sup> EC Photovoltaic Solar Energy Conference, James & James Ltd., (2000).

[3] R. Ebner, M. Radike, J. Summhammer, V. Schlosser, this conference.

[4] M. Radike, J. Summhammer, Solar Energy Material & Solar Cells, **65**, (2001) 303.